Speed development at freeway curves based on high frequency floating car data

Vos, Johan; Farah, Haneen

DOI
10.18757/ejtir.2022.22.2.6114

Publication date
2022

Document Version
Final published version

Published in
European Journal of Transport and Infrastructure Research

Issue 22(2), 2022, pp. 201-223
https://doi.org/10.18757/ejtir.2022.22.2.6114

TU Delft OPEN

EJTIR

ISSN: 1567-7141
http://ejtir.tudelft.nl/

Speed development at freeway curves based on high frequency floating car data

Johan Vos[1]
Department of Transport and Planning, Delft University of Technology, the Netherlands.

Haneen Farah[2]
Department of Transport and Planning, Delft University of Technology, the Netherlands.

Road designers need to have insights where deceleration and acceleration are expected related to the position of the curve, and in in which amount so that drivers are able to safely decelerate and accelerate respectively into and out of a freeway curve. For this, empirical speed data is needed. Therefore, Floating Car Data in 153 curves in The Netherlands were collected at a resolution of 1 Hz and were filtered on free-flow periods, to analyse over 800 thousand unique continuous free-flow speed observations on these curves. Regression models were developed to predict speed development, including deceleration and acceleration behaviour upon entering and exiting freeway curves. The models rely on easy to generate geometric design variables, including the start and end position of the horizontal curve, the horizontal radius and the number of lanes. Using these variables, the designer can predict the speed development based on the 85th percentile of speed and acceleration, relative to the position of the curve. The regression models reveal strong goodness-of-fit of the predicted 85th percentiles of speed in a curve, showing acceleration and deceleration inside the curve, and higher predicted 85th percentile speeds than the design speeds. The models also show satisfying results in speed development prediction in sets of consecutive curves with different characteristics, as well as deceleration when entering a first curve and acceleration when exiting a last curve. These insights are valuable in evaluating road design in relation to traffic safety based on its predicted use.

Keywords: *85th percentile speed, acceleration, freeway curves, high frequency floating car data, road design*

Publishing history

Submitted: 19 October 2021
Accepted: 23 June 2022
Published: 24 June 2022

Cite as

Vos, J., & Farah, H. (2022). Speed development at freeway curves based on high frequency floating car data. European Journal of Transport and Infrastructure Research, 22(2), 201-223.

[1] A: Department of Transport and Planning, Delft University of Technology, P.O. Box 5048, 2600 GA Delft, the Netherlands.E: j.vos-1@tudelft.nl
[2] A: Department of Transport and Planning, Delft University of Technology, P.O. Box 5048, 2600 GA Delft, the Netherlands.E: h.farah@tudelft.nl

1. Introduction

Curves are known as an infrastructural element where many road accidents occur (Davidse, Duijvenvoorde, & Louwerse, 2020). If a curve comes unexpectedly, drivers might be surprised (Alexander & Lunenfeld, 1986; Richard & Lichty, 2013) and react by braking too fiercely resulting in large speed differences in traffic or a skidding car and run-of-the-road accidents (Aarts & Van Schagen, 2006; Mahapatra & Kumar, 2018; Torbic et al., 2014). Drivers should be able to safely decelerate and accelerate respectively into and out of a freeway curve. Therefore designers need to have insights in where deceleration and acceleration are expected related to the position of the curve, and in in which amount. This will help designers to design safe deceleration and accelerations lanes, so the driver can give the needed attention to the operational driving task at hand; speed adjustment. It will furthermore give insights into the smoothness of speed adjustment in consecutive curves, leading to a consistent design without surprising the driver (Hassan, 2004).

Traditionally, speed prediction modelling use point speed data, but it has been argued that this method does not show enough insights into acceleration and deceleration (Hassan, Sarhan, & Dimaiuta, 2011). Continuous speed profiles however do provide valuable insights into speed development along curves (Dias, Oguchi, & Wimalasena, 2018), because they provide continuous information along the alignment. In the last decade several studies have generated speed profiles using driving simulators (Bella, 2014; Montella, Galante, Imbriani, Mauriello, & Pernetti, 2014; Montella, Galante, Mauriello, & Aria, 2015; Wang, Guo, & Tarko, 2020), usually to research specific elements of the road (Bobermin, Silva, & Ferreira, 2021). Other studies used instrumented vehicles to analyse speed profiles (Altamira, García Ramírez, Echaveguren, & Marcet, 2014; Cafiso & Cerni, 2012; Cafiso & La Cava, 2009; Echaveguren, Henríquez, & Jiménez-Ramos, 2020; Hashim, Abdel-Wahed, & Moustafa, 2016; Malaghan, Pawar, & Dia, 2020, 2021; Montella, Pariota, Galante, Imbriani, & Mauriello, 2014; Nama, Sil, Maurya, & Maji, 2020). These methods usually have low sample sizes of observed curves or participants and suffer from participant bias. Furthermore, besides the study of Montella et al. (2015), these studies focus on the amount of deceleration or acceleration, but not on where this is located related to the position of the curve. **Error! Reference source not found.** shows the general approach and the used variables in recent literature. Usually, the minimum speed in the curve (v_{min}) is identified and subtracted from the maximum speed upstream of the curve (v_{max}). This results in the speed difference known as Δv. The distance between the positions of v_{max} and v_{min} (D) is then used to calculate the deceleration (d) using formula 1.

$$d = \frac{(v_{max} - v_{min})}{2D} = \frac{\Delta v}{2D} \quad (1)$$

where

d	=	average deceleration
v_{max}	=	maximum measured speed upstream of curve
v_{min}	=	minimum measured speed inside curve
Δv	=	the difference between v_{max} and v_{min}
D	=	distance between positions of v_{max} and v_{min}

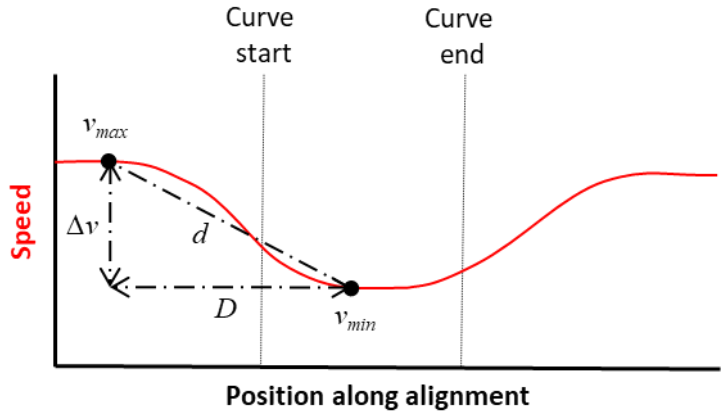

Figure 1. Overview of general approach and variables used in recent deceleration research.

This approach has two drawbacks. It does not generate a model to position the deceleration related to the position of the curve, and it assumes a constant deceleration. Several studies have shown that v_{min} is not reached at curve start, otherwise known as the Point of Curvature (*PC*), or at the Midpoint of the Curve (*MC*) (Bella, 2014; Malaghan et al., 2021; Vos, Farah, & Hagenzieker, 2021). So, there seems to be no geometrically fixed point defining v_{min}. This makes it hard to implement speed profiles in geometric design checks and could underestimate the combined need for lateral and longitudinal friction during curve entry (Hassan, 2004). To summarize, previous research into speed profiles has improved our understanding of deceleration. However, there are still some limitations in existing speed profile research:

- low sample sizes;
- participant bias;
- inability to relate deceleration to position of curve;
- an assumption of constant deceleration based on Δv.

Therefore, we aim to further develop the understanding of speed behaviour and its implementation by developing speed and acceleration profiles. This research therefore has three goals:

1. model speed development related to the position of the curve as speed profiles;
2. model acceleration development related to the position of the curve as acceleration profiles;
3. use generic variables which are easy to derive from geometric designs and develop parsimonious models (Tenenbaum & Filho, 2016).

To overcome the low sample sizes and participant bias, High Frequency Floating Car Data (HF FCD) is used. This is speed data collected from a route navigation app users which was for our study set to a data sampling frequency of 1 Hz. This approach ensures naturalistic driving, because the users of the app were unaware of the data collection. The only downside is that the users remain completely anonymous, because of General Data Protection Regulation laws, so no demographics are known. Besides this downside, this data collection provides thousands of unique speed profiles in a large number of curves.

To our knowledge, this study is the first to use HF FCD to analyse speed profiles and generate models to predict deceleration and acceleration related to the position of the curve.

The following section further discusses the methods. The third section analyses the retrieved data in two parts; first it analyses the speed development, followed by the acceleration development. In the fourth section we discuss the results and the study limitations. Finally, we summarize the main conclusions in section five.

2. Methods

For the analysis in this study, 99 freeway sections in The Netherlands were selected, containing 153 curves with different characteristics, as shown in Table 1. The freeway sections were chosen with upstream and downstream tangents of at least 1.000 m, which ensure that drivers are able to drive their desired operating speed in free flow situations. The curves are located throughout The Netherlands – both in rural and urban areas – as shown in Figure 2, and only contain main carriageways and connector roads in junctions. The selected curves include long tangents upstream and downstream which ensure that drivers' speed behaviours are not influenced by other geometric elements such as small tangents, or cross roads.

Figure 2. Map of The Netherlands showing the selected freeway sections.

All selected road sections in this study were re-engineered based on digital terrain models to obtain the present geometrical characteristics. The main horizontal characteristics are summarised in Table 1. Since The Netherlands is a rather flat country, the range of the vertical grades of the curves is -3.3% – +2.8% (average 0.0%, SD = 1.1%).

2.1 High Frequency Floating Car Data

High Frequency Floating Car Data (HF FCD) was collected by setting the data collection frequency of the route navigation app "Flitsmeister" to 1 Hz along the selected freeway sections. This smartphone app is used by approximately 1.6 million users in The Netherlands – roughly 15% of all driver-licence holders. Data was collected in March, April and September of 2020, generating 12.5 million individual speed profiles. These were bought by the Dutch Ministry of Infrastructure. The HF FCD was then mapped along the re-engineered freeway sections, to generate individual

speed and acceleration profiles, which are connected to the geometric characteristics of the respective road sections.

In these individual speed profiles, breakpoints (BPs) were identified. These BPs are the positions surrounding curve start and curve end where drivers deviate from a constant speed (Montella et al., 2015; Vos et al., 2021). These BPs are defined based on the position where drivers first deviate from 0 m/s² upstream of curve start (BP1), first reset to 0 m/s² downstream of curve start (BP2), first deviate from 0 m/s² upstream of a curve end (BP3), and first reset to 0 m/s² downstream of a curve end (BP4). Furthermore, we defined the positions where maximum deceleration occurs upstream of curve start (MAXdec) and where the maximum acceleration occurs downstream of curve end (MAXacc). This is shown in Figure 3, in theoretical speed and acceleration profiles. Curve start and curve end are therefore the reference points (i.e, distance value of zero) of the BPs and are defined by the start and end of the continuous radius. Relative to these reference points, upstream position values are negative and downstream position values are positive. At those positions, the speed and deceleration are captured for the models in this research.

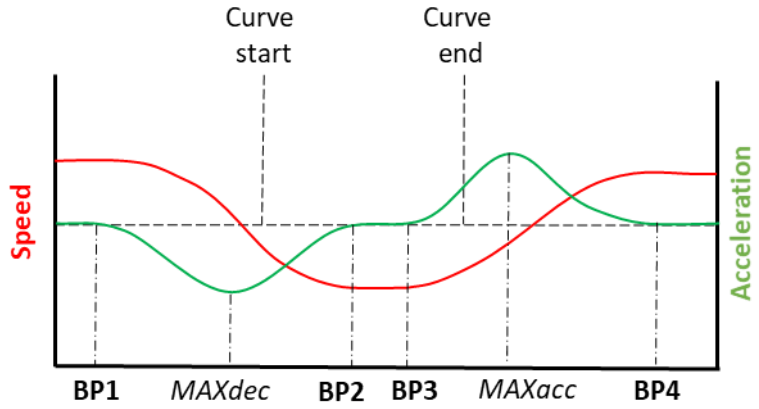

Figure 3. Theoretical speed and acceleration profiles, showing the positions of the breakpoints and maximum deceleration and acceleration in relation to curve start and curve end.

2.2 Data filtering and curve grouping

Individual speed profiles during road works and in non free-flow situations were filtered out, because these speed observations could be affected by other factors other than the road geometrics. Furthermore, v85 is usually defined as the speed which 85 percent of all vehicles are observed to travel at or below in free-flowing conditions (Hassan, Sarhan, Porter, et al., 2011; Lamm, Choueiri, Hayward, & Paluri, 1988). For simplicity we will refer to the 85th percentile of the free flow measurements as 85th percentile speeds or v85. To identify free-flow observations, detector loop data (Nationaal Dataportaal Wegverkeer, 2020) was used from each freeway section which shows the total amount of traffic per minute per lane. Based on the timestamps of the HF FCD, we eliminated all individual speed profiles in periods with more than 5 vehicles per minute per lane. This results in a 95% probability that the remaining individual speed observations were in free flow situation with headways greater than 5 seconds (Hashim, 2011). After filtering, the data included 881,153 individual speed profiles, with an average of 8,901 individual speed profiles per freeway section (max 39,618, min 330). This sample represents 7.6% off all drivers in the selected time periods (free-flow without roadworks). The loop-detectors also collect average speed per minute. The averages of the entire population from the loop-detectors were compared, to the speed observations from the HF FCD data sample and this has shown that the sample of drivers in the HF FCD drive on average 5.4 km/h (SD 4.9 km/h) faster than the entire population. Based on other speed observations of the entire population (Farah, Daamen, & Hoogendoorn, 2019), the sample in this study represents on average around the 60th percentile of all drivers.

Because in the selected freeway sections several consecutive curves were included, the curves were grouped based on their relative positions. This was done to gain information about the speed and

acceleration observations at the different BPs without it being influenced by other nearby consecutive curves. So, speed behaviour upstream of a curve was analysed on first curves only, speed inside a curve was analysed on single curves only and speed downstream of a curve was analysed on last curves only. Single curves are also included in the first and last curve groups, because it is assumed they have the same behaviour at respectively curve start and curve end. The variables for each curve group are summarised in Table 1.

Table 1. Summary of the curve groups

	All curves	First curves	Single curves	Last curves
Number of curves	153	99	47	99
Average radius (m.)	297 range: 60 – 801 SD = 174	315 range: 60 – 801 SD = 189	301 range: 60 – 749 SD = 172	268 range: 60 – 750 SD = 167
Average length (m.)	303 range: 31 – 1018 SD = 210	308 range: 31 – 1018 SD = 223	432 range: 78 – 1018 SD = 212	338 range: 50 – 1018 SD = 212
Average deflection angle (grad.)	86 range: 6 – 284 SD = 67	85 range: 6 – 284 SD = 71	112 range: 36 – 284 SD = 65	103 range: 11 – 284 SD = 68
Mode of number of lanes	1 range: 1 – 4 SD = 0.8	1 range: 1 – 4 SD = 0.8	1 range: 1 – 3 SD = 0.7	1 range: 1 – 3 SD = 0.6

Based on these curve groups speed development was analysed first, followed by an analysis on acceleration development.

3. Data analysis

The focus of the analysis in this paper is on the 85th percentile of speed and acceleration because design speeds are determined based on the 85th percentile of speeds or anticipated operating speeds (Fitzpatrick & Kahl, 1992; *A Policy on Geometric Design of Highways and Streets 2018*, 2018; *ROA*, 2019). Furthermore, the main design variable in a horizontal curve, is it's horizontal radius which is known to be of main influence on driving speeds (Hassan, Sarhan, Porter, et al., 2011). Therefore, the speed analysis starts with analysing the 85th percentile of speeds at the different breakpoints and in relation to the horizontal radius.

3.1 Speed profiles based on the 85th percentile of speed

The 85th percentile of speeds at the four breakpoints of each curve in the dataset were calculated, but also at the curve start and curve end. The deceleration and acceleration inside the continuous curve is of special interest, because this could entail risks of skidding since this combines both the use of both lateral and longitudinal friction (Himes, Porter, Hamilton, & Donnell, 2019; Pacejka & Besselink, 2012). Furthermore the 50th percentile of the positions of the four breakpoints relative to curve start and curve end were calculated, because the aim is to generate 85th percentile speed profiles using these positions. The distribution of the positions of breakpoints (boxplots in Figure 4) is rather similar along the different speed percentiles, as shown in Figure 4. So, using the 15th or 85th percentile positions, would result in skewed profiles, meaning the presented deceleration or acceleration would be too steep or to flat.

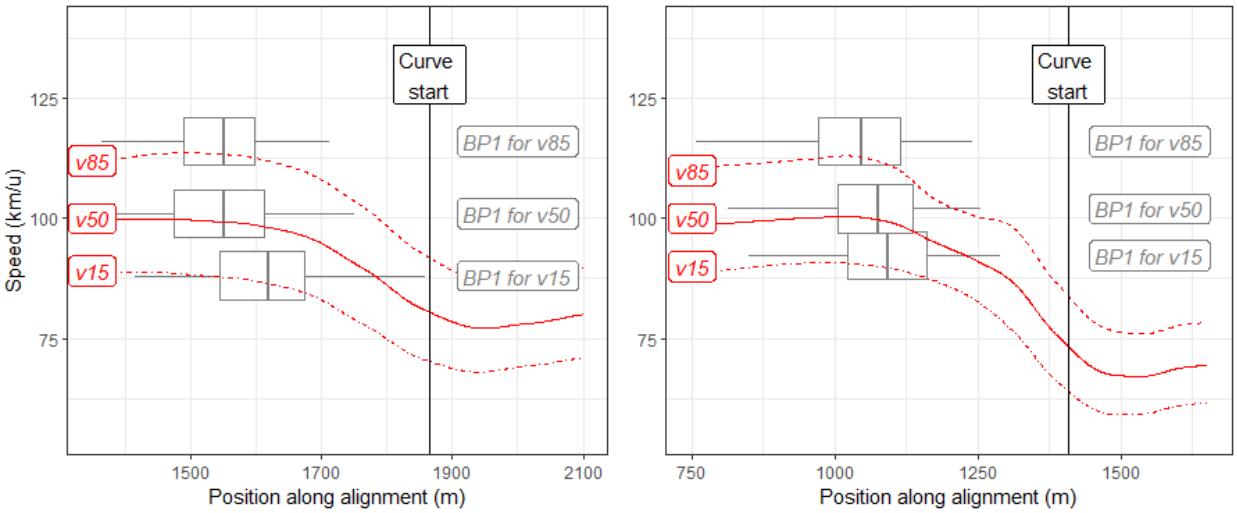

Figure 4. Two examples showing the 15th, 50th and 85th speed profile, and their respective distributions of positions of BP1 and the position of curve start along the alignment.

The values for the *v85* and positions of the breakpoints are plotted in Figure 5, shown in relation to the horizontal radius of the curve. The grey points represent all the 153 curves in the dataset, the black points represent the specific group used. The used groups show a lesser variability than the entire set, which is to be expected.

Figure 5A shows how drivers tend to start braking more ahead of a curve ($pos50_{BP1}$), when the radius decreases. This makes sense, because a greater amount of speed has to be reduced. Figure 5B shows a rather very mild increase in speed at BP1 ($v85_{BP1}$) with a mean of 124 km/h, which is to be expected, since no major influence of the curve is expected here because relative long tangents are positioned upstream of the first curves. The slight slope towards smaller radii can be explained by the fact that some small radii in The Netherlands are designed on separated carriageways in junctions, which tend to have lower speeds. Figures 5C, 5E, 5G and 5H show a firm correlation of speed throughout the curves, at curve start, BP2, BP3 and curve end ($v85_{CS}$, $v85_{BP2}$, $v85_{BP3}$ and $v85_{CE}$) to the horizontal radius, respectively. Figures 5D and 5F show a weak correlation of the position where drivers stop decelerating in a curve ($pos50_{BP2}$) and start accelerating out of a curve ($pos50_{BP3}$). These positions are however rather constant at around 75 m. after curve start for BP2 and 75 m. before curve end for BP3. Figure 5I shows it takes drivers longer to gain a constant speed after leaving curves ($v85_{BP4}$) with lower radii, which is explained by the greater speed increase. Lastly, Figure 5J shows that drivers adopt a lower speed after leaving a curve with a small radius at BP4 ($pos85_{BP4}$) than when they leave a curve with a relative large radius.

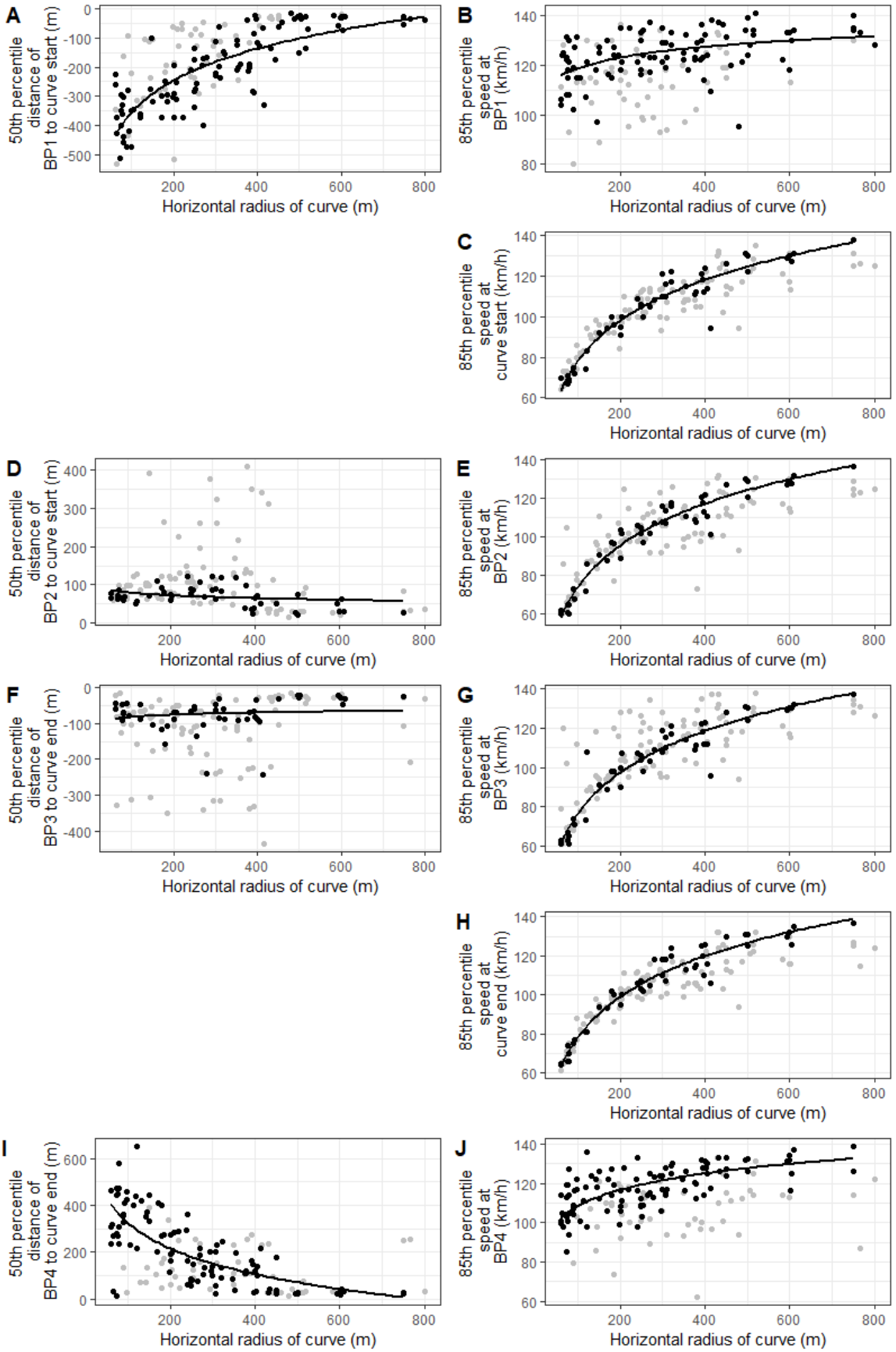

Figure 5. Scatterplots comparing horizontal radius to the 85th percentile of speed and median positions of breakpoints. All 153 curves are represented in grey points. The used subset in black points refer in A and B to first curves, C through H to single curves, and for I and J to last curves.

The regression lines shown in Figure 5 can be used to calculate coordinates of speed profiles based on horizontal radii. For example, using Figure 5A for the position of BP1 and Figure 5B for the 85th percentile of speed at BP1, it can be determined where drivers start to decelerate upstream of curve start and at which speed. In Figure 6 these coordinates were calculated for a set of horizontal radii to generate speed profiles based on breakpoints. Figure 6A shows the speed profiles for different horizontal radii upon curve entry, based on the following coordinates: ($pos50_{BP1}$, $v85_{BP1}$), (0, $v85_{CS}$), ($pos50_{BP2}$, $v85_{BP2}$). Figure 6B shows the speed profiles for different horizontal radii upon curve exit, based on the following coordinates: ($pos50_{BP3}$, $v85_{BP3}$), (0, $v85_{CE}$), ($pos50_{BP4}$, $v85_{BP4}$). Figure 6A shows deceleration slopes, which get steeper if the radius decreases below 300, meaning drivers brake harder in front of relative small radii. The opposite is true for acceleration out of a curve. Figure 6B shows that the acceleration is rather constant out of a curve, but decreases when radii increase over 300 m. Furthermore, Figure 6 shows that deceleration and acceleration is greater upstream and downstream of the curve respectively, than inside a curve.

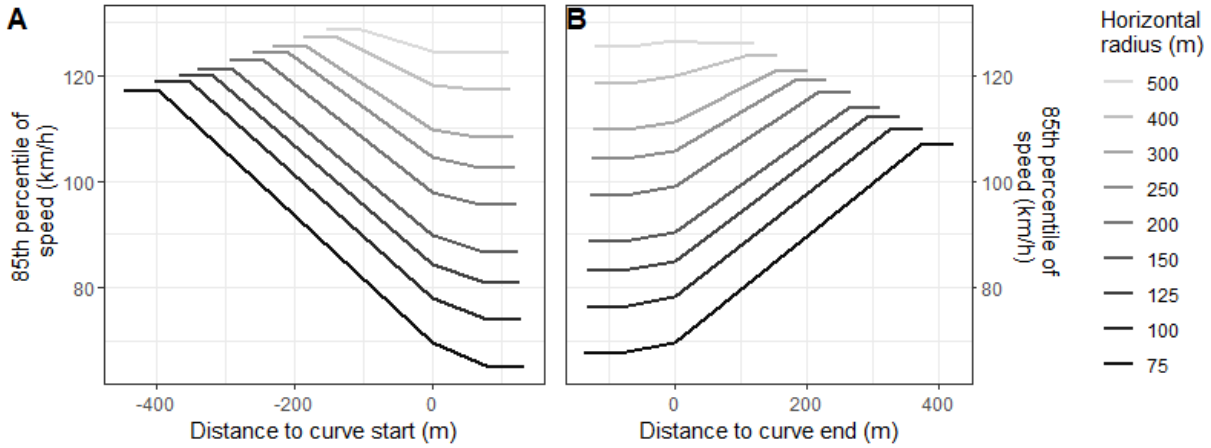

Figure 6. Profiles for the 85th percentile of speeds on different horizontal radii based on breakpoints and related to the start and end of the curve.

However, as seen in Figure 5, there is still some variability in the speed profiles as shown in Figure 6. A sensitivity analysis was done on which variables could explain this variability best. Using variables which are customary in design guidelines, and are easily distinguishable by drivers (Vos, Farah, & Hagenzieker, 2020), the influence of the number of lanes and the length of the curve were identified as extra factors explaining these variabilities. Figure 7A shows how the 85th percentile speed differs when having 1 lane in a curve compared to more lanes (notice that the regression lines for 2 and 3 lanes overlap). Figure 7B shows higher speeds in curve lengths shorter than 250 m. Appendix A contains the different subsets of these variables for the 85th percentile speeds, and for the positions of the breakpoints.

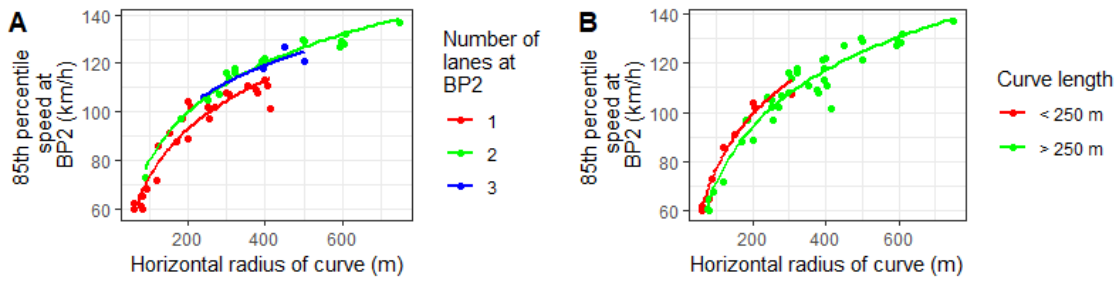

Figure 7. Sensitivity analysis on the number of lanes and length of a curve.

Adding the distinction between 1 lane or more to the model improved all the *v85* predictions significantly ($p < 0.001$). Collinearity between variables was checked, for example the distinction between 1 lane or more was not found to be correlated with $\ln(R_h)$ and was therefore used in the models. The correlation of $nLanes1_{BP1}$ with $\ln(R_h)$ is $r = 0.09$, for *nLanes1* is $r = 0.35$ and for $nLanes1_{BP4}$ is $r = -0.04$. For the positions of BP1 and BP4, adding extra variables did not result in better models. The models for the positions of BP2 and BP3 are very weak, and adding variables did not improve models significantly, so, to keep in line with BP1 and BP4 we chose not to add variables. Adding the curve length itself or the distinction of curve length being more or less than 250 meters only improved the *v85* predictions at BP2 and BP3. To create a continuous speed profile, the predictions from all speed and position models need to be combined. Adding curve length variables only in BP2 and BP3 models would mean that continuous speed profiles use different variables at different positions resulting in misalignments of speed prediction between CS and BP2, and BP3 and CE. So this variable was excluded for all breakpoints. This resulted in modelled speed profiles which align the observed data better, by using the below presented best subsets of variables to predict the coordinates of speed profiles. The coordinates are in the form of (*pos50*, *v85*) for each breakpoint.

$pos50_{BP1} = 155 * \ln(R_h) - 1067$ ($R^2 = 0.679$) (2)

$pos50_{BP2} = -11 * \ln(R_h) + 130$ ($R^2 = 0.078$) (3)

$pos50_{BP3} = 9 * \ln(R_h) - 122$ ($R^2 = 0.015$) (4)

$pos50_{BP4} = -159 * \ln(R_h) + 1057$ ($R^2 = 0.531$) (5)

$v85_{BP1} = 6 * \ln(R_h) + 4 * nLanes1_{BP1} + 88$ ($R^2 = 0.220$) (6)

$v85_{CS} = 26 * \ln(R_h) + 8 * nLanes1 - 41$ ($R^2 = 0.948$) (7)

$v85_{BP2} = 28 * \ln(R_h) + 7 * nLanes1 - 58$ ($R^2 = 0.961$) (8)

$v85_{BP3} = 27 * \ln(R_h) + 7 * nLanes1 - 51$ ($R^2 = 0.919$) (9)

$v85_{CE} = 27 * \ln(R_h) + 8 * nLanes1 - 47$ ($R^2 = 0.971$) (10)

$v85_{BP4} = 58 * \ln(R_h) + 4 * nLanes1_{BP4} + 58$ ($R^2 = 0.423$) (11)

where:

pos50 = 50th percentile of a position relative to curve start or curve end (distance in m.);

v85 = 85th percentile of speed (km/h);

R_h = horizontal radius of the curve (m.);

nLanes1 = distinction of having 1 or more lanes (0 = 1 lane, 1 = more lanes).

The R^2 of the different models show that the radius of the curve and the number of lanes explain well the variability in the speed inside a curve. The variability of the positions of BP1 and BP4 is moderately explained by the radius of the curve. The variability of speed at BP1 and BP4 is weakly explained by curve radius and number of lanes at these BPs, this is generally seen for speed prediction models on tangents (Hassan, Sarhan, Porter, et al., 2011). The mean speed at BP1 with more than 1 lane is 125 km/h (SD = 9.3 km/h). The radius of the curve does not explain well the variability observed in the positions of BP2 and BP3, but, as seen in Figure 4D and 4F, the positions of these points are rather constant and not influenced by the radius of the curve. $d50_{BP2}$ has a mean of 93 m. (SD = 72 m) and $d50_{BP3}$ has a mean of -106 m. (SD = 94 m.). Both have a median of 76 m. (negative for $d50_{BP3}$).

These models were compared on actual speed profiles to see how well they align with speed development in different situations. In Figure 8 actual observed 85th percentile speed profiles are shown in a red dashed lines. The different horizontal radii and positions of curve start (*CS*) and curve end (*CE*) were added, together with the number of lanes in relation to the speed profile. For each curve, a predicted speed profile based on the following coordinates ((*pos50*$_{BP1}$ + *CS*), *v85*$_{BP1}$), (*CS*, *v85*$_{CS}$), ((*pos50*$_{BP2}$ + *CS*), *v85*$_{BP2}$), ((*pos50*$_{BP3}$ + *CE*), *v85*$_{BP3}$), (*CE*, *v85*$_{CE}$), ((*pos50*$_{BP4}$ + *CE*), *v85*$_{BP4}$) was added. Figure 8A shows a single, relative sharp, curve. The predicted profile aligns well with both slopes, but we notice also deceleration upstream of BP1 and acceleration downstream of BP4, although being at a lesser slope. Figure 8B shows predictions of a set of curves with radii around 500 m. Only marginal speed development is seen and predicted. Figure 8C shows a set of curves with decreasing radii. The predictions follow the actual slope of entering the set of curves and exiting the set of curves. It also shows to negate the coordinates for BP3 to BP4 from the first curve and BP1 of the second, since they are smoothed together. Figure 8D shows this in a more extreme setting with two relative small radii curves, connected with a small tangent. Observed slopes of exiting the first curve and entering the second are quite well aligned with the predicted slopes. Figure 8E shows a set of three curves, of which the first two have about the same radius, and the last one is larger. The slope of entering the first curve of the set is quit smooth in the observed red line, but aligns about half way with the predicted line. Exiting the curve combination of curves was predicted at a steeper slope towards the third curve. Possibly drivers remain cautious towards the last curve. Finally, Figure 8F shows a complex road section with two sets of curves with each two curves and different numbers of lanes. In the tangent between the two sets of curves, a higher speed is predicted, but overall, the slopes are pretty well aligned with the observed speed. Overall, Figure 8 shows relative well alignment of predicted and observed speeds in the curves, as well as the slopes of acceleration and deceleration, but are less well aligned with speeds at tangents. It also shows that based on the predicted speeds, inconsistent designs can be revealed, because these designs do not show a smooth operating speed profile.

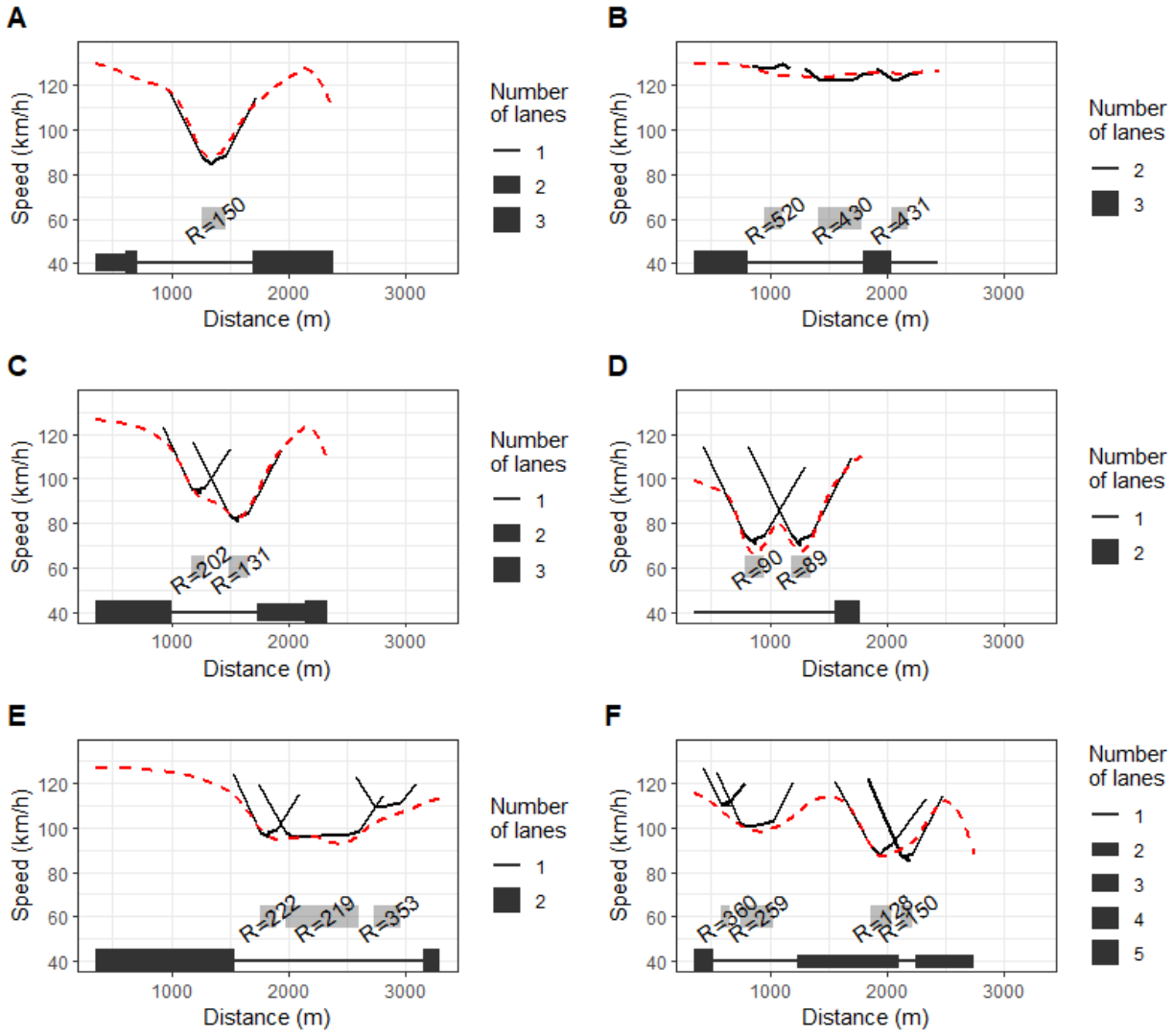

Figure 8. Observed and predicted speed profiles; red dashed line is the observed 85th percentile speed, the black lines are the predicted speed profiles per curve. Curve radii in a grey box representing the position of the curve. Below that a line indicating the number of lanes present along the profile.

In Figure 8, it was shown that the slopes that were predicted using the coordinates for the BPs and their respective 85th percentile speeds are rather accurate. So, based on these coordinates, the average acceleration and decelerations based on the different slopes can be calculated. Table 2 provides the outcomes of those calculations for the range of radii shown in Figure 6. As noticed in Figure 6, Table 2 shows rather constant decelerations and accelerations along the range of radii up to 250 meters. Larger radii seem to result in lower accelerations and decelerations. The exception is the deceleration from *CS* to BP1, which shows to increase with decreasing radii.

Table 2. Average decelerations and accelerations based on predicted slopes from 85th percentile speed profiles

R_h (m.)	1 lane				2 or more lanes			
	Deceleration		Acceleration		Deceleration		Acceleration	
	BP1-CS (m/s²)	CS-BP2 (m/s²)	BP3-CE (m/s²)	CE-BP4 (m/s²)	BP1-CS (m/s²)	CS-BP2 (m/s²)	BP3-CE (m/s²)	CE-BP4 (m/s²)
75	-0.77	-0.29	0.12	0.61	-0.76	-0.40	0.18	0.57
100	-0.80	-0.29	0.13	0.64	-0.76	-0.39	0.19	0.58
125	-0.81	-0.27	0.13	0.65	-0.76	-0.38	0.20	0.58
150	-0.81	-0.25	0.13	0.66	-0.75	-0.37	0.20	0.57
200	-0.81	-0.20	0.13	0.66	-0.72	-0.33	0.21	0.53
250	-0.79	-0.16	0.13	0.66	-0.67	-0.29	0.22	0.48
300	-0.76	-0.11	0.13	0.63	-0.61	-0.25	0.22	0.41
400	-0.67	-0.02	0.13	0.54	-0.44	-0.16	0.22	0.19
500	-0.51	0.07	0.12	0.35	-0.18	-0.08	0.22	-0.22

3.2 Acceleration profiles based on the 85th percentile of deceleration and acceleration

In the previous paragraph the main focus was on analysing the slope in speed profiles to gain insights into deceleration and acceleration upon curve entry and curve exit. This paragraph enriches these insights, using the median positions where drivers maximize their decelerations and accelerations ($pos50_{MAXdec}$, $pos50_{MAXacc}$) and the observed 85th percentile of respectively the deceleration and acceleration ($a85_{MAXdec}$, $a85_{MAXacc}$) at those positions. This provides insights into the development of accelerations. Since the average acceleration inside of curves was found to be different from the average acceleration upstream and downstream a curve, the 85th percentile of deceleration and acceleration observed at respectively curve start and curve end ($a85_{CS}$, $a85_{CE}$) were also extracted from the data.

Figure 9 shows scatterplots of these variables in relation to the horizontal radius. Figure 9A shows that drivers tend to maximise their deceleration closer to the curve start when the radius is larger, and Figure 9B shows that drivers decelerate harder at that point and when the radius is smaller, which is the same for the deceleration at curve start, but in a lesser amount, as shown in Figure 9C. Figure 9D shows that at curve end acceleration out of a curve is faster when the radius is smaller. Acceleration is highest at a position after curve end, and gets closer to curve end as the radius gets larger, as shown in Figure 9E. Finally, Figure 9F shows that at that point of maximum acceleration, the acceleration is larger when the radius decreases.

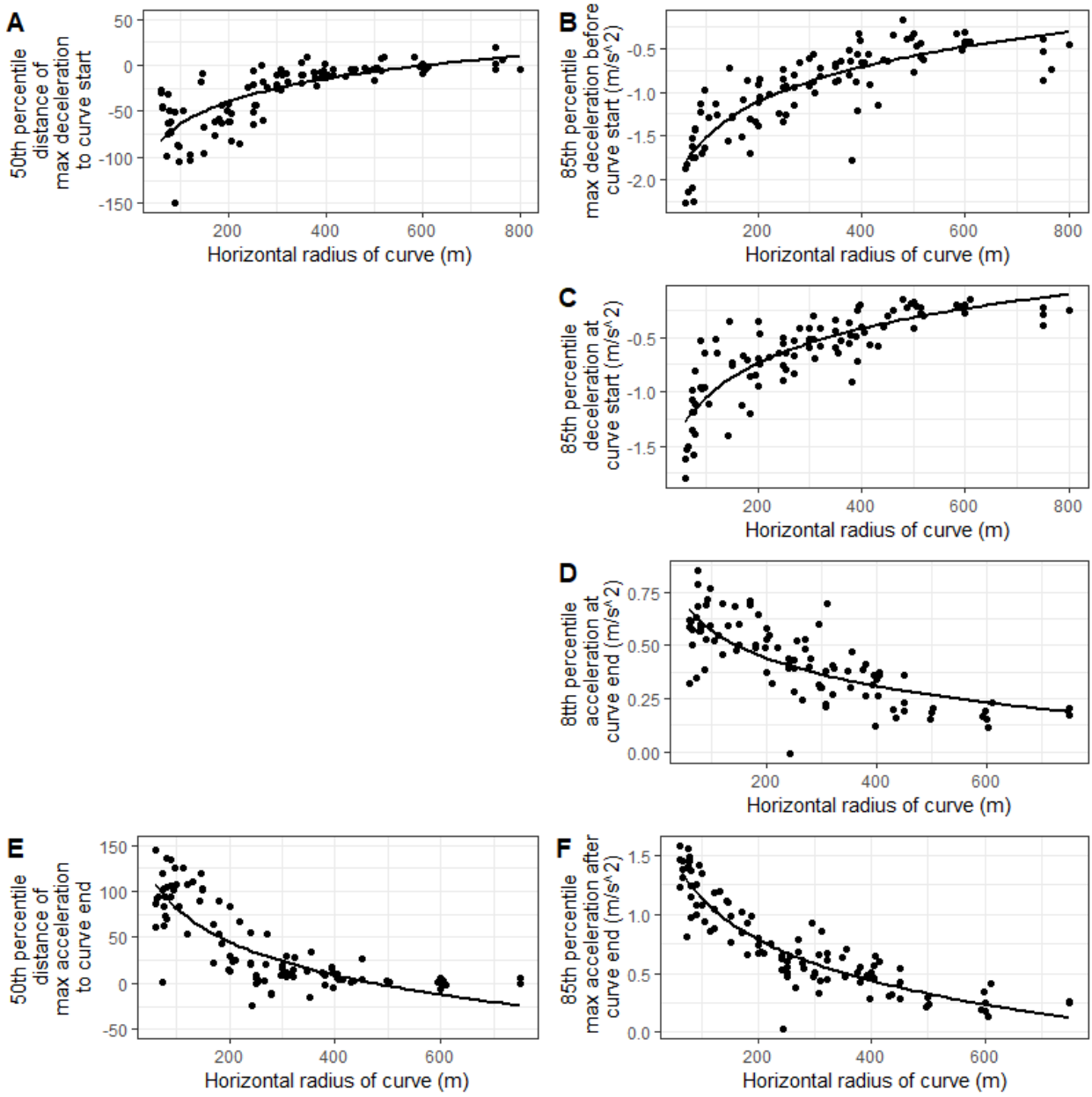

Figure 9. Scatterplots comparing horizontal radius to the 85th percentile of acceleration and deceleration as well as the positions of maximum acceleration and deceleration

Breakpoints are defined based on the acceleration being 0 m/s² at those positions (Figure 3), so *pos50* (50th percentile of those positions) for each breakpoint can be used as a position in an acceleration profile where 0 m/s² is observed. By adding information from the regression lines in Figure 8, a deceleration and acceleration profile can be plotted based on the positions of the breakpoints, maximum acceleration, curve start and curve end. Figure 10 shows these acceleration profiles for the same set of horizontal radii used in Figure 6. Figure 10A shows the deceleration profiles upon curve entry based on the following coordinates: ($pos50_{BP1}$, 0), ($pos50_{MAXdec}$, $a85_{MAXdec}$), (0, $a85_{CS}$), ($pos50_{BP2}$, 0). Figure 10B shows the acceleration profiles upon curve exit based on the following coordinates: ($pos50_{BP3}$, 0), ($pos50_{MAXacc}$, $a85_{MAXacc}$), (0, $a85_{CE}$), ($pos50_{BP4}$, 0). Overall, Figure 10 shows the deceleration and acceleration development upstream and downstream of a curve.

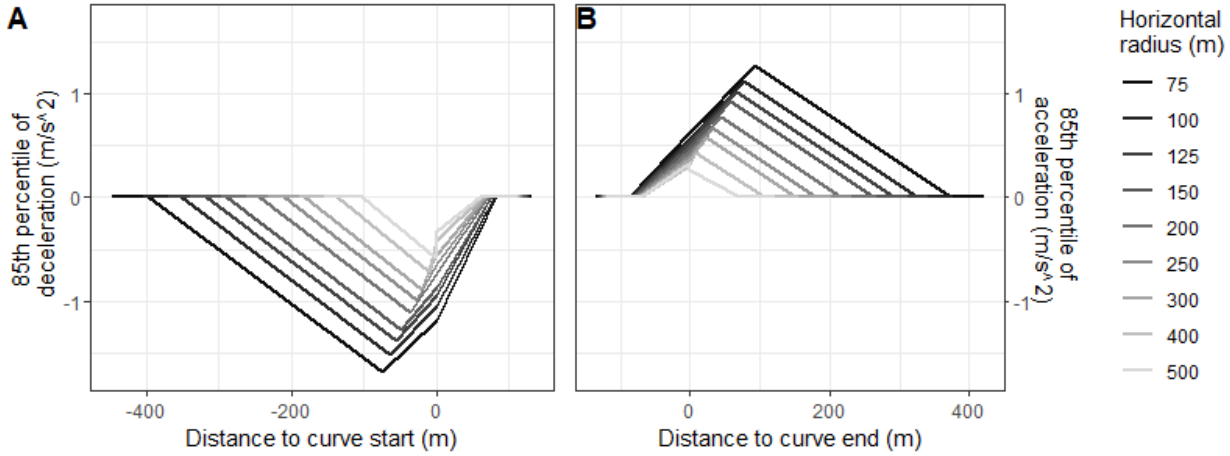

Figure 10. Profiles for the 85th percentile of deceleration and acceleration on different horizontal radii based on breakpoints and maximum acceleration

Because Figure 9 shows variability around the regression lines, it was explored which variables might explain this variability. However, none of the variables added to the models contributed significantly to explaining this variability for the acceleration models. Appendix B shows the tested models. To keep in line with the other models for the 50th percentile of positions, no other variables were added to the positions of maximum deceleration and acceleration. The best subsets of variables for the additional coordinates needed for acceleration and deceleration profiles are given below:

$$pos50_{MAXdec} = 39 * \ln(R_h) - 241 \quad (R^2 = 0.351) \quad (12)$$

$$pos50_{MAXacc} = -49 * \ln(R_h) + 307 \quad (R^2 = 0.518) \quad (13)$$

$$a85_{MAXdec} = -0.58 * \ln(R_h) - 4.18 \quad (R^2 = 0.712) \quad (14)$$

$$a85_{CS} = -0.46 * \ln(R_h) - 3.15 \quad (R^2 = 0.702) \quad (15)$$

$$a85_{CE} = -0.19 * \ln(R_h) + 1.46 \quad (R^2 = 0.702) \quad (16)$$

$$a85_{MAXacc} = -0.50 * \ln(R_h) + 3.44 \quad (R^2 = 0.825) \quad (17)$$

where

pos50 = 50th percentile of a position relative to curve start or curve end (distance in m.);

a85 = 85th percentile of acceleration (m/s²);

R_h = horizontal radius of the curve (m.).

The R^2 values reveal relatively strong goodness-of-fit of the predicted 85th percentiles of deceleration and acceleration, while the goodness-of-fit of the models predicting positions of maximum deceleration and acceleration are relatively weak.

These models were compared on actual acceleration and deceleration profiles, taken from the same road sections as Figure 8. In Figure 10 the 15th percentile and 85th percentile of acceleration were plotted in green dashed lines. The 15th percentile of acceleration is used as the 85th percentile of deceleration. The start and end of each curve was also included. Based on these positions of the curves, the predicted acceleration profiles per curve were created based on the following coordinates: $((pos50_{BP1} + CS), 0)$, $((pos50_{MAXdec} + CS), a85_{MAXdec})$, $(CS, a85_{CS})$, $((pos50_{BP2} + CS), 0)$, $((pos50_{BP3} + CE), 0)$, $(CE, a85_{CE})$, $((pos50_{MAXdacc} + CE), a85_{MAXacc})$, $((pos50_{BP4} + CE), 0)$. Figure 11A

shows a relative good match to the deceleration and acceleration around a single curve. Figure 11B shows that the predicted acceleration and decelerations of curves with radii around 500 meter are not detectable by the 15th and 85th percentiles of observed acceleration. Figure 11C shows that with a set of curves, only the deceleration up to the first curve, and the acceleration after the last curve are aligned well. Between the two curves, the acceleration remains rather neutral, because speed was already adjusted in the first curve. Figure 11D shows that if the curves are a bit more apart, parts of the acceleration and deceleration between the curves are aligned, but with an offset. Figure 11E shows how the model aligns the acceleration upstream of the third curve relatively well, based on de acceleration out of the second curve. Figure 11F finally, shows how the deceleration before the second set of curves is aligned relatively well, based on the tangent between both sets of curves. In general, Figure 11 shows acceleration profiles are relatively well aligned for curves surrounded by tangents. For sets of curves, only the deceleration into the first curve, and acceleration out of the last curve are relatively well aligned. The acceleration profile between consecutive curves should be examined based on the speed profile mostly; if the speed remains relatively the same, no acceleration is observed.

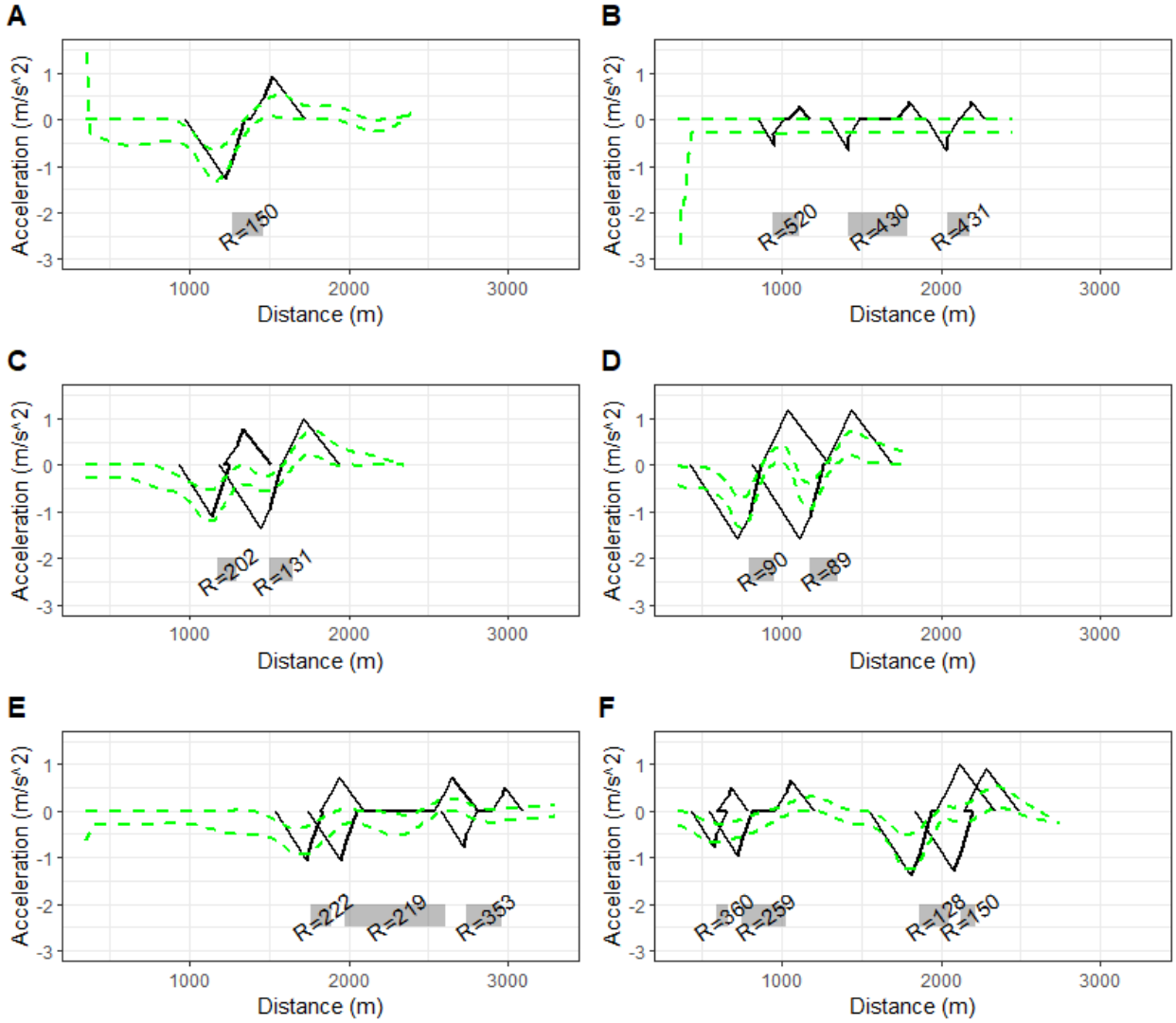

Figure 11. Observed and predicted acceleration profiles; green dashed lines are the observed accelerations at 15th and 85th percentile, the black lines are the predicted acceleration profiles per curve. Curve radii in a grey box representing the position of the curve. These acceleration profiles are taken from the same curves as presented in Figure 7

4. Discussion and limitations

The strong correlation between the horizontal radius to speed and acceleration is confirmed, which is also shown in numerous other studies (Farah et al., 2019; Hassan, Sarhan, Porter, et al., 2011). When identifying the slopes in the speed profiles when entering a curve, the results show different findings from those by Montella et al. (2015) where increasing slopes were found when the radius decreases. This study found a relation only between the radius of the curve and the 85th percentile of maximum decelerations, not to the average decelerations.

Also in line with other studies, this study was unable to present strong correlations between the speed on tangents and the geometric elements. The speed on tangents upstream of a curve are of importance to predict the deceleration before the curve. The predicted slopes in speed profiles are generally well aligned with the observed slopes, which are the average deceleration calculated based on speeds on tangents and in the curve.

The acceleration models show a lesser goodness of fit than the speed models. This could be explained because acceleration is treated as a derivative of speed in this research. The slopes of the acceleration models were not further investigated, because of increasing uncertainties in the derivations. The slope of acceleration is known as the longitudinal jerk (m/s^3) and has limited influence on general traffic safety, but can be used to identify individual aggressive drivers (Feng et al., 2017).

It was the aim of this study to include only variables which are easily extracted from a geometric design, namely horizontal radius, start and end position of curves, and the number of lanes. Other, more complex variables (Vos et al., 2021), might improve the models further, but are harder to implement in design evaluations. Furthermore, variables such as type of roadway, superelevation, transition curves, Curvature Change Rate or weather conditions don't have significant impact on speed behaviour or are collinear to horizontal radius (Vos et al., 2021).

The length of a curve was omitted from the regression models, as it was shown in the analysis to be insignificant for predicting the speeds at breakpoint outside of the curve. The models however show acceleration and deceleration inside a curve. So, with shorter curve-lengths acceleration and deceleration will overlap and visually show unrealistic speed development. This predicts a higher speed inside a curve then predicted by $v85_{BP2}$ and $v85_{BP3}$. More research is needed to understand the smoothing of the profiles, based on the current insights of the breakpoints.

The 85th percentile of observed speeds before drivers start to decelerate upstream of a curve confirm the selected design speed of 120 km/h for main carriageways with two or more lanes. Based on the 85th percentile of speeds observed inside the curves, we noticed discrepancies up to 30 km/h towards the design speeds used for designing freeway curves in The Netherlands (*ROA*, 2019). These insights can be used to evaluate safety risks which arise from these discrepancies, such as friction demand, sight distances both horizontally and vertically, forgiving shoulder design, etcetera.

The regression models shown in this study are based on radii ranging from 60 to 800 meters. It was noticed that when radii larger than 500 meters are used in these models, unrealistically high values are predicted. It seems the 85th percentile speed and acceleration are only influenced by radii smaller than 500 meters.

Since the sample of drivers in this study showed to drive on average 5.4 km/h faster over the loop detectors, it is assumed that the 85th percentile speeds shown and predicted in this study, are lower for the entire population.

5. Conclusions

Insights were gained in this study on speed and acceleration development upstream and downstream of freeway curves based on a highly detailed data-set containing High Frequency Floating Car Data combined with re-engineered road sections and detector loop data. Slopes in predicted speed models, as well as predicted maximum deceleration and acceleration, based on the horizontal radius and number of available lanes align well with the observed speed and acceleration data. Furthermore, distinction between acceleration outside and inside a curve was made, which is of importance to design evaluation related to friction. We show that inside a curve besides lateral friction, also longitudinal friction is absorbed. This deviates from design guidelines in which only lateral friction is used to calculate curve radii. Differences in deceleration and acceleration patterns outside and inside the curve are observed, with decreasing curve radii, drivers decelerate stronger in a curve.

Speed and acceleration development are predicted based on the coordinates of breakpoints. Breakpoints identify positions relative to curve start and curve end where drivers start and stop accelerating. Combining these positions with the 85th percentile of speed, speed development can be predicted. It is shown that the speed development in a curve can be strongly explained by the horizontal radius and whether the curve has one or more lanes. The correlations to the speed development on the tangents were weaker, but the predicted slopes in the speed profiles (which represent deceleration or acceleration) align well with the observed speed development. Furthermore, the speed development around consecutive curves is reasonably well predictable, using the developed predictive models per curve, gaining insights into speed development by their overlapping characteristics. Acceleration development was further investigated by gaining insight into the positions where maximum deceleration and acceleration is reached and the 85th percentile of those observations. The observed acceleration profiles for entering a first curve and exiting a last curve also align reasonably well to the predicted acceleration development. Acceleration inside a set of curves is not predictable based on our models, because our models assume acceleration outside of a curve, while a follow-up curve might not induce this.

The presented models are ready to be implemented into geometric design evaluation, because they show how speed and acceleration develops based on the position of the curve. Furthermore, the models can give insights into the needed acceleration and deceleration lengths around relative sharp curves in freeway connector roads. Because the speed development can be predicted, designers can check the needed sight distances, signage or even the needed friction, as well as speed inconsistencies.

The presented speed observations confirm the design speed on main carriageways based on the 85th percentile of observed speed. The design speeds in curves however do not match up with the observed 85th percentile of speed in this study confirming similar findings of previous studies.

Acknowledgements

The authors would like to thank the executive agency of the Dutch Ministry of Infrastructure and Water Management (Rijkswaterstaat) for making this research possible.

References

Aarts, L., & Van Schagen, I. (2006). Driving speed and the risk of road crashes: A review. *Accident Analysis and Prevention, 38*(2), 215-224. doi:10.1016/j.aap.2005.07.004

Alexander, G. J., & Lunenfeld, H. (1986). *Driver expectancy in highway design and traffic operations*: US Department of Transportation, Federal Highway Administration, Office of Traffic Operations.

Altamira, A., García Ramírez, Y., Echaveguren, T., & Marcet, J. (2014). *Acceleration and Deceleration Patterns on Horizontal Curves and Their Tangents on Two-Lane Rural Roads*. Paper presented at the Transportation Research Board 93rd Annual Meeting, Washington.

Bella, F. (2014). Driver Performance Approaching and Departing Curves: Driving Simulator Study. *Traffic Injury Prevention, 15*(3), 310-318. doi:10.1080/15389588.2013.813022

Bobermin, M. P., Silva, M. M., & Ferreira, S. (2021). Driving simulators to evaluate road geometric design effects on driver behaviour: A systematic review. *Accident Analysis & Prevention, 150*, 105923. doi:https://doi.org/10.1016/j.aap.2020.105923

Cafiso, S., & Cerni, G. (2012). New approach to defining continuous speed profile models for two-lane rural roads. *Transportation Research Record*(2309), 157-167. doi:10.3141/2309-16

Cafiso, S., & La Cava, G. (2009) Driving performance, alignment consistency, and road safety. In. *Transportation Research Record* (pp. 1-8).

Davidse, R. J., Duijvenvoorde, K. v., & Louwerse, W. J. R. (2020). Fatal road crashes on national roads in 2019; Analysis of crash and injury factors and resulting potential countermeasures. *SWOV, Leidschendam*(R-2020-29), 45.

Dias, C., Oguchi, T., & Wimalasena, K. (2018). Drivers' Speeding Behavior on Expressway Curves: Exploring the Effect of Curve Radius and Desired Speed. *Transportation Research Record, 2672*, 48 –60. doi:10.1177/0361198118778931

Echaveguren, T., Henríquez, C., & Jiménez-Ramos, G. (2020). Longitudinal acceleration models for horizontal reverse curves of two-lane rural roads. *Baltic Journal of Road and Bridge Engineering, 15*(1), 103-125. doi:10.7250/bjrbe.2020-15.463

Farah, H., Daamen, W., & Hoogendoorn, S. (2019). How do drivers negotiate horizontal ramp curves in system interchanges in the Netherlands? *Safety Science, 119*, 58-69. doi:10.1016/j.ssci.2018.09.016

Feng, F., Bao, S., Sayer, J. R., Flannagan, C., Manser, M., & Wunderlich, R. (2017). Can vehicle longitudinal jerk be used to identify aggressive drivers? An examination using naturalistic driving data. *Accident Analysis & Prevention, 104*, 125-136. doi:https://doi.org/10.1016/j.aap.2017.04.012

Fitzpatrick, K., & Kahl, K. (1992). *A Historical and Literature Review of Horizontal Curve Design*. Austin, Texas: Texas Transportation Institute.

Hashim, I. H. (2011). Analysis of speed characteristics for rural two-lane roads: A field study from Minoufiya Governorate, Egypt. *Ain Shams Engineering Journal, 2*(1), 43-52. doi:https://doi.org/10.1016/j.asej.2011.05.005

Hashim, I. H., Abdel-Wahed, T. A., & Moustafa, Y. (2016). Toward an operating speed profile model for rural two-lane roads in Egypt. *Journal of Traffic and Transportation Engineering (English Edition), 3*(1), 82-88. doi:10.1016/j.jtte.2015.09.005

Hassan, Y. (2004). Highway design consistency: Refining the state of knowledge and practice. *Transportation Research Record*(1881), 63-71. doi:10.3141/1881-08

Hassan, Y., Sarhan, M., & Dimaiuta, M. (2011). Deficiencies in Existing Speed Models. In *Modeling Operating Speed: Synthesis Report*. Washington, D.C.: Transportation Research Board.

Hassan, Y., Sarhan, M., Porter, R., Dimaiuta, M., Donnell, E., Garcia, A., . . . Taylor, M. (2011). *Modeling Operating Speed: Synthesis Report*. Washington, D.C.: Transportation Research Board.

Himes, S., Porter, R. J., Hamilton, I., & Donnell, E. (2019). Safety Evaluation of Geometric Design Criteria: Horizontal Curve Radius and Side Friction Demand on Rural, Two-Lane Highways. *Transportation Research Record, 2673*, 516-525. doi:10.1177/0361198119835514

Lamm, R., Choueiri, E. M., Hayward, J. C., & Paluri, A. (1988). Possible design procedure to promote design consistency in highway geometric design on two-lane rural roads. *Transportation Research Record, 1195*, 111.

Mahapatra, G., & Kumar, A. M. (2018). Defining driving behaviour using friction-circle concept: An experimental study. *European Transport - Trasporti Europei*(67).

Malaghan, V., Pawar, D. S., & Dia, H. (2020). Modeling Operating Speed Using Continuous Speed Profiles on Two-Lane Rural Highways in India. *Journal of Transportation Engineering Part A: Systems, 146*(11). doi:10.1061/JTEPBS.0000447

Malaghan, V., Pawar, D. S., & Dia, H. (2021). Modeling Acceleration and Deceleration Rates for Two-Lane Rural Highways Using Global Positioning System Data. *Journal of Advanced Transportation, 2021*. doi:10.1155/2021/6630876

Montella, A., Galante, F., Imbriani, L. L., Mauriello, F., & Pernetti, M. (2014). Simulator evaluation of drivers' behaviour on horizontal curves of two-lane rural highways. *Advances in Transportation Studies*(34), 91-104.

Montella, A., Galante, F., Mauriello, F., & Aria, M. (2015). Continuous Speed Profiles to Investigate Drivers' Behavior on Two-Lane Rural Highways. *Transportation Research Record, 2521*(1), 3-11.

Montella, A., Pariota, L., Galante, F., Imbriani, L. L., & Mauriello, F. (2014) Prediction of drivers' speed behavior on rural motorways based on an instrumented vehicle study. In*: Vol. 2434. Transportation Research Record* (pp. 52-62).

Nama, S., Sil, G., Maurya, A. K., & Maji, A. (2020) Acceleration and Deceleration Behavior in Departing and Approaching Sections of Curve Using Naturalistic Driving Data. In*: Vol. 69. Lecture Notes in Civil Engineering* (pp. 693-704).

Nationaal Dataportaal Wegverkeer. (2020). Retrieved from: https://www.ndw.nu/

Pacejka, H., & Besselink, I. J. M. (2012). *Tire and Vehicle Dynamics*: Elsevier Science & Technology.

A Policy on Geometric Design of Highways and Streets 2018. (2018). Washington, D.C.: AASHTO.

Richard, C. M., & Lichty, M. G. (2013). *Driver Expectations When Navigating Complex Interchanges* (FHWA-HRT-13-048). Retrieved from Georgetown Pike:

ROA - Richtlijn Ontwerp Autosnelwegen 2019. (2019). (Rijkswaterstaat Ed.). Utrecht: Rijkswaterstaat - Grote Projecten en Onderhoud.

Tenenbaum, G., & Filho, E. (2016). Chapter 3 - Measurement Considerations in Performance Psychology. In M. Raab, B. Lobinger, S. Hoffmann, A. Pizzera, & S. Laborde (Eds.), *Performance Psychology* (pp. 31-44). San Diego: Academic Press.

Torbic, D. J., Donnell, E. T., Brennan, S. N., Brown, A., O'Laughlin, M. K., & Bauer, K. M. (2014) Superelevation design for sharp horizontal curves on steep grades. In*: Vol. 2436. Transportation Research Record* (pp. 81-91).

Vos, J., Farah, H., & Hagenzieker, M. (2020). How do dutch drivers perceive horizontal curves on freeway interchanges and which cues influence their speed choice? *IATSS Research*. doi:https://doi.org/10.1016/j.iatssr.2020.11.004

Vos, J., Farah, H., & Hagenzieker, M. (2021). Speed behaviour upon approaching freeway curves. *Accident Analysis & Prevention, 159*, 106276. doi:https://doi.org/10.1016/j.aap.2021.106276

Wang, X., Guo, Q., & Tarko, A. P. (2020). Modeling speed profiles on mountainous freeways using high resolution data. *Transportation Research Part C: Emerging Technologies, 117*. doi:10.1016/j.trc.2020.102679

Appendix A

Table 3. Developed regression models for 85th percentile speeds

	$v85_{BP1}$	$v85_{BP1}$	$v85_{BP1}$	$v85_{BP1}$	$v85_{CS}$	$v85_{CS}$	$v85_{CS}$	$v85_{CS}$	$v85_{BP2}$	$v85_{BP2}$	$v85_{BP2}$	$v85_{BP2}$	$v85_{BP3}$	$v85_{BP3}$	$v85_{BP3}$	$v85_{BP3}$	$v85_{CE}$	$v85_{CE}$	$v85_{CE}$	$v85_{CE}$	$v85_{BP4}$	$v85_{BP4}$	$v85_{BP4}$	$v85_{BP4}$
Constant	90.38***	88.42***	88.73***	89.87***	-55.33***	-41.34***	-43.28***	-45.69***	-70.04***	-57.74***	-62.12***	-65.33***	-63.69***	-50.87***	-56.58***	-59.88***	-60.57***	-46.65***	-46.37***	-46.73***	63.16***	58.49***	58.57***	62.11***
	(6.55)	(6.63)	(6.65)	(6.72)	(7.05)	(6.41)	(6.54)	(6.79)	(6.40)	(5.92)	(5.43)	(5.71)	(8.48)	(8.55)	(8.03)	(8.61)	(6.06)	(4.98)	(5.17)	(5.45)	(6.80)	(7.14)	(7.30)	(7.61)
ln(Rh)	6.13***	5.78***	5.59***	5.22***	28.95***	25.76***	26.48***	27.09***	31.28***	28.47***	30.11***	30.80***	30.40***	27.47***	29.61***	30.24***	30.12***	26.94***	26.84***	26.97***	10.12***	10.45***	10.43***	9.43***
	(1.17)	(1.19)	(1.21)	(1.27)	(1.27)	(1.22)	(1.34)	(1.44)	(1.15)	(1.13)	(1.11)	(1.21)	(1.53)	(1.63)	(1.64)	(1.82)	(1.09)	(0.95)	(1.06)	(1.15)	(1.26)	(1.25)	(1.33)	(1.46)
$nLanes1_{BP1}$		4.34	4.45	4.54																				
		(2.79)	(2.80)	(2.79)																				
nLanes1						8.11***	8.28***	8.95***		7.13***	7.50***	8.58***		7.43**	7.91***	9.15***		8.07***	8.05***	8.09***				
						(1.66)	(1.65)	(1.70)		(1.53)	(1.37)	(1.43)		(2.21)	(2.03)	(2.15)		(1.29)	(1.31)	(1.36)				
$nLanes1_{BP4}$																						3.83+	3.82+	3.45+
																						(2.00)	(2.01)	(2.01)
length > 250m			1.34				-2.65				-5.98**				-7.79**				0.38				0.11	
			(1.69)				(2.05)				(1.70)				(2.52)				(1.62)				(1.85)	
length in m.				0.00				-0.01+				-0.01**				-0.02**				0.00				0.01
				(0.00)				(0.00)				(0.00)				(0.01)				(0.00)				(0.00)
Num.Obs.	99	99	99	99	47	47	47	47	47	47	47	47	47	47	47	47	47	47	47	47	99	99	99	99
R2	0.220	0.239	0.244	0.250	0.920	0.948	0.950	0.952	0.942	0.961	0.970	0.970	0.898	0.919	0.934	0.931	0.944	0.971	0.971	0.971	0.401	0.423	0.423	0.434
R2 Adj.	0.212	0.223	0.220	0.227	0.919	0.946	0.947	0.948	0.941	0.960	0.968	0.968	0.896	0.915	0.929	0.926	0.943	0.969	0.968	0.968	0.395	0.411	0.405	0.416
AIC	703.6	703.1	704.5	703.6	303.7	285.3	285.6	284.3	294.6	277.8	268.0	268.0	321.1	312.3	304.9	306.6	289.5	261.6	263.5	263.6	712.6	710.9	712.9	711.1
BIC	711.4	713.5	717.4	716.6	309.3	292.7	294.8	293.6	300.2	285.2	277.2	277.3	326.6	319.7	314.1	315.9	295.1	269.0	272.8	272.8	720.4	721.3	725.9	724.1
Log.Lik.	-348.790	-347.563	-347.236	-346.801	-148.872	-138.670	-137.775	-137.159	-144.318	-134.906	-128.985	-129.003	-157.528	-152.152	-147.436	-148.324	-141.771	-126.784	-126.754	-126.783	-353.323	-351.466	-351.464	-350.546
F	27.296	15.052	10.206	10.575	519.801	404.235	274.137	281.800	736.472	548.251	463.636	463.269	396.592	249.383	201.770	193.755	761.151	723.764	472.155	471.563	64.962	35.211	23.231	24.259

+ p < 0.1, * p < 0.05, ** p < 0.01, *** p < 0.001

Table 4. Developed regression models for 50th percentile of positions of breakpoints

	$pos50_{BP1}$	$pos50_{BP1}$	$pos50_{BP1}$	$pos50_{BP1}$	$pos50_{BP2}$	$pos50_{BP2}$	$pos50_{BP2}$	$pos50_{BP2}$	$pos50_{BP2}$	$pos50_{BP3}$	$pos50_{BP3}$	$pos50_{BP3}$	$pos50_{BP3}$	$pos50_{BP3}$	$pos50_{BP4}$	$pos50_{BP4}$	$pos50_{BP4}$	$pos50_{BP4}$
Constant	-1066.77***	-1051.49***	-1060.96***	-1041.97***	130.41***	123.97**	145.66***	113.41**	85.32***	-122.18*	-89.72	-151.06*	-130.20+	-80.70***	1057.18***	1025.45***	1059.37***	1052.67***
	(60.43)	(61.33)	(60.29)	(60.47)	(31.36)	(35.36)	(32.14)	(36.35)	(8.69)	(56.60)	(63.01)	(57.83)	(66.21)	(15.82)	(82.05)	(87.23)	(83.76)	(87.37)
ln(Rh)	155.10***	157.83***	152.16***	146.28***	-11.04+	-9.57	-16.48*	-6.15		8.53	1.11	18.83	10.84		-158.66***	-156.38***	-159.43***	-157.25***
	(10.83)	(10.99)	(10.99)	(11.41)	(5.65)	(6.74)	(6.45)	(7.72)		(10.19)	(12.01)	(11.61)	(14.07)		(15.14)	(15.28)	(16.07)	(17.71)
$nLanes1_{BP1}$		-33.84																
		(25.87)																
nLanes1						-3.73					18.83							
						(9.15)					(16.30)							
$nLanes1_{BP4}$																26.04		
																(24.43)		
length > *250m*			21.53				18.22					-34.50+					3.37	
			(15.59)				(11.06)					(19.90)					(22.58)	
length in m.				0.08*				-0.02	-0.04*				-0.01	0.01				-0.01
				(0.04)				(0.02)	(0.02)				(0.05)	(0.03)				(0.06)
Num.Obs.	99	99	99	99	47	47	47	47	47	47	47	47	47	47	99	99	99	99
R2	0.679	0.685	0.685	0.694	0.078	0.082	0.132	0.096	0.083	0.015	0.044	0.078	0.017	0.003	0.531	0.536	0.531	0.531
R2 Adj.	0.676	0.678	0.679	0.687	0.058	0.040	0.092	0.055	0.063	-0.007	0.001	0.036	-0.028	-0.019	0.526	0.527	0.521	0.521
AIC	1143.5	1143.7	1143.5	1140.9	444.0	445.8	443.2	445.1	443.7	499.5	500.1	498.4	501.4	500.1	1205.7	1206.6	1207.7	1207.7
BIC	1151.3	1154.1	1153.9	1151.3	449.5	453.2	450.6	452.5	449.3	505.1	507.5	505.8	508.8	505.6	1213.5	1217.0	1218.1	1218.1
Log.Lik.	-568.747	-567.872	-567.773	-566.441	-218.993	-218.904	-217.586	-218.537	-218.873	-246.754	-246.052	-245.201	-246.723	-247.038	-599.873	-599.291	-599.862	-599.861
F	205.094	104.155	104.459	108.617	3.824	1.960	3.342	2.337	4.073	0.700	1.020	1.869	0.372	0.152	109.754	55.522	54.335	54.337

+ p < 0.1, * p < 0.05, ** p < 0.01, *** p < 0.001

Appendix B

Table 5. Developed regression models for 85th percentile of acceleration

	$a85_{MAXdec}$	$a85_{MAXdec}$	$a85_{MAXdec}$	$a85_{MAXdec}$	$a85_{CS}$	$a85_{CS}$	$a85_{CS}$	$a85_{CS}$	$a85_{CE}$	$a85_{CE}$	$a85_{CE}$	$a85_{CE}$	$a85_{MAXacc}$	$a85_{MAXacc}$	$a85_{MAXacc}$	$a85_{MAXacc}$
Constant	-4.18***	-4.21***	-4.17***	-4.12***	-3.15***	-3.13***	-3.15***	-3.12***	1.46***	1.45***	1.47***	1.44***	3.44***	3.40***	3.45***	3.45***
	(0.21)	(0.23)	(0.21)	(0.21)	(0.17)	(0.19)	(0.17)	(0.17)	(0.10)	(0.10)	(0.10)	(0.10)	(0.13)	(0.13)	(0.13)	(0.13)
ln(Rh)	0.58***	0.59***	0.57***	0.56***	0.46***	0.45***	0.45***	0.44***	-0.19***	-0.19***	-0.20***	-0.19***	-0.50***	-0.49***	-0.51***	-0.51***
	(0.04)	(0.04)	(0.04)	(0.04)	(0.03)	(0.04)	(0.03)	(0.03)	(0.02)	(0.02)	(0.02)	(0.02)	(0.02)	(0.02)	(0.02)	(0.03)
nLanes1		-0.02				0.02				-0.01				-0.05		
		(0.06)				(0.05)				(0.03)				(0.03)		
length > 250 m			0.04				0.00				0.02				0.02	
			(0.05)				(0.04)				(0.03)				(0.03)	
length in m.				0.00				0.00				0.00				0.00
				(0.00)				(0.00)				(0.00)				(0.00)
Num.Obs.	99	99	99	99	96	96	96	96	96	96	96	96	99	99	99	99
R2	0.712	0.712	0.714	0.720	0.702	0.703	0.702	0.706	0.543	0.544	0.545	0.545	0.827	0.831	0.827	0.827
R2 Adj.	0.709	0.706	0.708	0.714	0.699	0.696	0.696	0.699	0.538	0.534	0.535	0.535	0.825	0.827	0.824	0.824
AIC	20.9	22.8	22.3	20.2	-22.8	-20.9	-20.8	-21.8	-126.3	-124.4	-124.7	-124.7	-76.8	-76.9	-75.0	-74.9
BIC	28.7	33.2	32.7	30.6	-15.1	-10.6	-10.5	-11.5	-118.6	-114.2	-114.5	-114.4	-69.0	-66.5	-64.7	-64.5
Log.Lik.	-7.467	-7.402	-7.167	-6.121	14.376	14.427	14.377	14.896	66.154	66.217	66.371	66.337	41.416	42.457	41.525	41.456
F	239.911	118.940	119.733	123.316	221.883	109.928	109.765	111.464	111.648	55.365	55.691	55.619	464.063	235.539	230.250	229.864

+ p < 0.1, * p < 0.05, ** p < 0.01, *** p < 0.001